International Journal of Pressure Vessels and Piping 209 (2024) 105161

Contents lists available at ScienceDirect

International Journal of Pressure Vessels and Piping

journal homepage: www.elsevier.com/locate/ijpvp

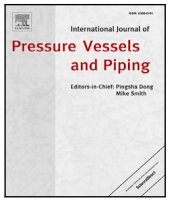

Model-experiment comparison of quasi static loading on a composite overwrap pressure vessel (Part 2)

Erick Montes de Oca Valle [a,*], S.M. Spearing [a], Ian Sinclair [a], Trevor Allen [a], Warren Hepples [b]

[a] University of Southampton, University Road, Southampton, SO17 1BJ, UK
[b] Luxfer Gas Cylinders, Colwick Industrial State, Nottingham NG4 2BH, UK

ARTICLE INFO

Keywords:
Finite element modelling
Pressure vessel
Cohesive elements
Damage tolerance

ABSTRACT

A methodology to develop a 3D Finite Element (FE) model of a full metal-lined Composite Overwrapped Pressure Vessel (COPV) was developed and is presented in this paper. The model is intended for prediction of the metal-composite delamination and residual dent depth developed in the metal liner as a result of quasi-static indentation loading. Cohesive elements are used to model the composite and the metal-composite interfaces. Experimental and numerical comparisons of force–displacement curves, delamination area and residual dent depth are presented. Numerical results are in good agreement to the experimental data.

1. Introduction

Composite Overwrapped Pressure Vessels (COPV) are hybrid structures that can contain gases usually in a range of 20 to 70 MPa. As such, these structures are used in applications such as self-contained breathing apparatus (SCBA), hydrogen storage, medical and transport [1]. Storage pressure, gas containment and weight minimization are the primary design criteria, damage tolerance is also an important consideration. As a result of out-of-plane loadings, including low velocity impacts (LVI), damage at the inner layers of the structure may occur, which complicates the integrity and load-carrying capacity assessment of the vessel after impact. Consequently, the effect subsequent damage may have on the structure's fatigue life is of great interest.

The effects of LVI in pressure vessels' performance has been widely reported in the literature. Wakayama et al. [2] performed LVI on several polymer-lined vessels with varied low-modulus pitch-based carbon fibres. Observations were made using Computer Tomography (CT) of the depth of damage resulting from using different impactor shapes in the tests. Results suggested that the depth of the damage is correlated with a reduction of the vessel's burst pressure. Similarly, Blanc-Vannet et al. investigated LVI on thick polymer-lined pressure vessels using different impact energies. It was reported that at higher impact energies the burst pressure of the vessel was significantly reduced. This is consistent with previous studies [3,4].

In addition to experimental testing, numerical modelling has been reported to be used to investigate damage tolerance in COPVs. Changliang et al. [5] developed a numerical model of metal-lined composite pressure vessels subjected to low velocity impact to investigate the damage occurring in the composite layers. This model was tested using empty and in-service pressurized cylinders. It was reported that the pressurized cylinder started to develop delamination and matrix cracking at impactor velocities lower than the empty cylinder. Although good correlation values were reported, only one value of pressure was used and no information regarding damage in the metal liner was reported. Han et al. [6] developed a 3D Finite Element (FE) model of a COPV in free fall drop test to investigate the extent of damage on the composite layers after impact. This model used Hashin's criterion to predict fibre fracture, matrix cracking and delamination under the impact region. This model was later used to simulate car-to-car collision and predict composite damage of the pressure vessel [7]. Although the model showed good agreement with experimental results, no clear definition of cylinder performance after impact was reported. Similar models using a ply-by-ply modelling approach have been also reported in literature, which focus on delamination within the CFRP layers or the separation between the composite plies and polymer liner [8,9].

The studies mentioned above focus on composite damage in pressure vessels as a result of LVI and the effect it has on damage tolerance. It has also been reported that some damage occurs in the liner, but only on polymer lined pressure vessels [8,10]. However, there has been a much less investigation of damage occurring in the metal liner, resulting from a LVI. Allen et al. [11] performed quasi-static indentation tests (as a proxy for LVI) on metal-lined composite pressure vessels and used CT to analyse the resultant damage. Results indicated that as a result of LVI there is a noticeable separation between the composite layers and the metal liner (Fig. 1). Force–displacement curves were obtained to analyse the overall structural response and compare it to the damage

* Corresponding author.
E-mail address: erick.montesdeocav@gmail.com (E. Montes de Oca Valle).

https://doi.org/10.1016/j.ijpvp.2024.105161
Received 21 June 2022; Received in revised form 18 February 2024; Accepted 22 February 2024
Available online 24 February 2024

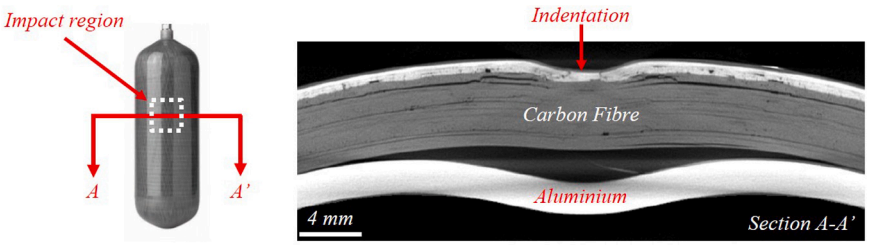

Fig. 1. CT image of metal-composite delamination within a COPV after quasi-static loading [11].

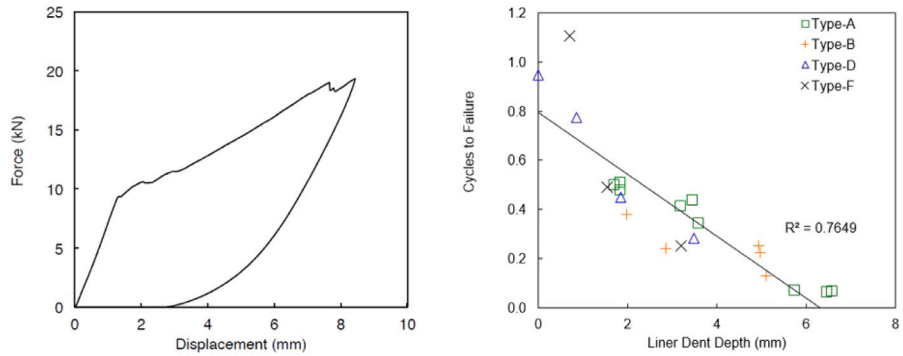

Fig. 2. COPV quasi-static loading behaviour: (a) Force–displacement curve response after indentation loading; (b) Correlation between liner dent depth and fatigue life [11].

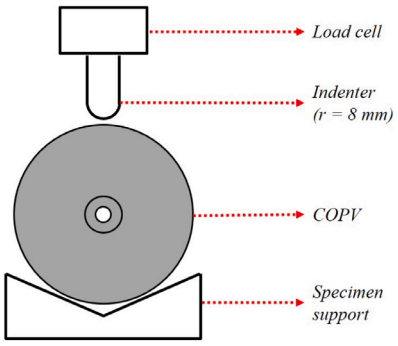

Fig. 3. Experimental set-up for COPV quasi-static indentation test [11].

progression at the metal-composite interface (Fig. 2a). Furthermore, damaged cylinders were subsequently tested for fatigue. Data suggested that there is a correlation between the depth of the dent and the post-impact fatigue life of the pressure vessel (Fig. 2b). However, due to the nature of the experiment, results could only be observed after load removal. Thus, further damage development investigations should be performed on the metal-liner.

This paper should be considered as a direct continuation of the methodology developed in [12]. This paper presents a 3D FE model to predict the indentation depth observed in the metal liner of a COPV as a result of quasi-static indentation. Cohesive elements previously defined are used to model composite and metal-composite interfaces. Four different vessel geometries were developed and compared to experimental force–displacement curves. Results are discussed in relation to geometric boundary conditions, simulation parameters and delamination regions.

Table 1
Type III cylinder models dimensions.

Name	Length [mm]	Outside diameter [mm]	Liner thickness [mm]	CFRP thickness [mm]	Cohesive layers
Model A	210	85	1.8	2.0	3
Model B	329	114	2.3	2.8	4
Model C	183	159	2.2	4.6	6
Model D	383	173	3.1	4.2	4

Table 2
Type III cylinder models running time @32 CPUs.

Model	Nodes	Elements	Solution time
Model A	78 803	42 214	20 h
Model B	139 165	78 130	23 h
Model D	435 695	239 843	+35 h

2. Methodology

2.1. Geometry and boundary conditions

COPV modelled in this work are similar in geometry and construction to those as presented in [13]. Specimen dimensions and number of cohesive layers used for each FE model are described in Table 1. Based on the results reported in previous work, Model C is used to develop the initial FE model and to investigate the validity of the numerical assumptions. Each of the cylinders tested experimentally was manufactured by Luxfer Gas Cylinders specifically for research purposes only, *i.e.* they were not intended for commercial use. Boundary conditions of the FE model are analogous to those defined by the experimental set up, in which the cylinder was located in a v-shaped support and indented using an electro-mechanical testing machine (see Fig. 3).

Material properties for the metal and the composite sections used for the model are 6061-T6 Aluminium and carbon fibre respectively. The

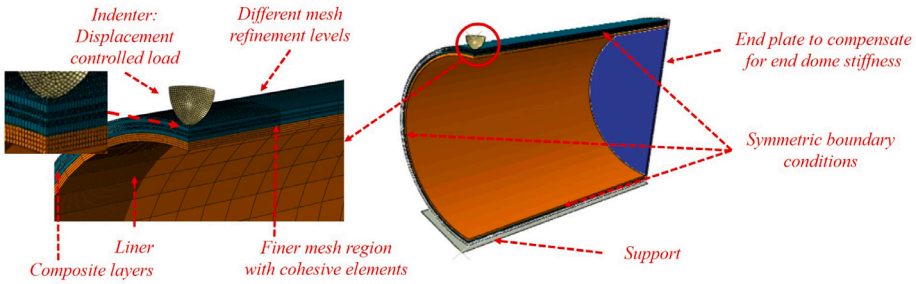

Fig. 4. Full cylinder FE model geometry, mesh and boundary conditions.

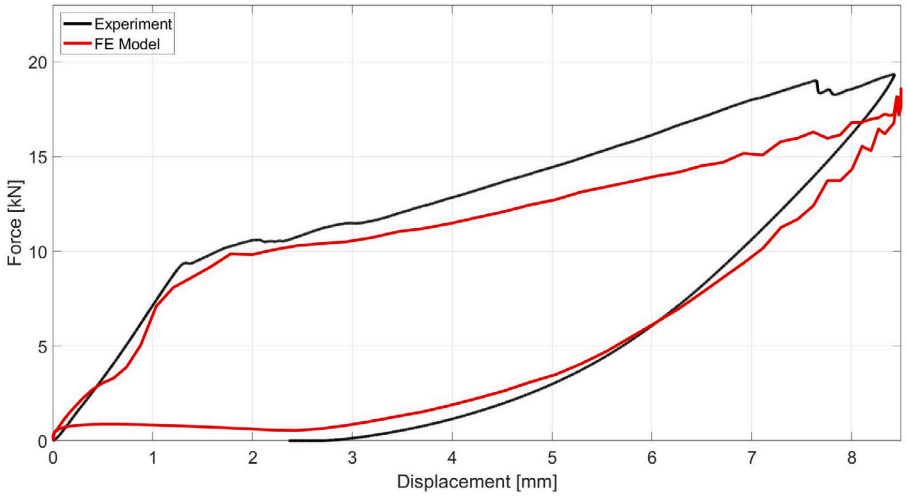

Fig. 5. Model C force–displacement curve, experimental vs. FE model results.

former is modelled as an elastic perfectly plastic material, whereas the latter is modelled as an elastic material. Both material properties used in the FE model are consistent to the ones observed in the experiments. Properties of the metal-liner interface were selected following the methodology defined in [12]. Several assumptions were taken to select the appropriate boundary conditions and reduce computational simulation time. For instance, some authors have reported the complexity of dome region modelling and the effect that the fibre alignment in this region has on the impact response directly to the dome [7,14]. However, this project investigates the damage response of the barrel section of the cylinder and, hence, it was assumed that the indentation is sufficiently far from the dome region so that it does not have a significant effect on the residual deformation prediction. Consequently, the dome region was not modelled in detail as reported, reducing the number of elements and interactions included in the simulation. In its place, a steel plate with equivalent stiffness properties was included in the model instead to match the initial structural stiffness.

Only 1/4 of the cylinder geometry was modelled along with symmetric boundary conditions to reduce computational time. The support is also modelled as a rigid body and $1/4^{th}$ of its geometry is used in consistency with the rest of the model. Similarly, the 8-mm hemispherical indenter is modelled as a rigid body due to the low level of deformation observed during the experiments in this component. The load is applied through enforced displacement of the indenter in two main steps: loading and unloading. The total displacement used in each step is 8.5 mm for Model C cylinder to be consistent with the analogous experiment reported in [11]. Fig. 4 shows a summary of the full cylinder FE model.

Regarding meshing parameters, the model was divided in two main regions, one which intends to be used as a geometrical boundary condition without any delamination and another which is expected to show delamination based on experimental observations. The former contains an average element size of 6 mm and the latter has a 0.6 mm element size. The finer mesh size was selected in such way so as to ensure that there are enough cohesive elements in the cohesive zone region [15]. The length of the finer section of the cylinder was selected as 30 mm, which is ≈ 20% of the geometry's total length. The model was developed using commercial software Abaqus/Explicit. Aluminium and composite sections are modelled using hexahedral solid elements (C3D8R) whereas the interfaces were modelled using solid cohesive elements (COH3D8). Total number of elements and nodes in the model is 133 165 and 247 944 respectively. It was run using the University of Southampton's Iridis super computer using 4 nodes in parallel with 8 CPU each. With this computing configuration total running time for this model was ≈27 h.

3. Results and discussion

3.1. Full cylinder vs. experimental comparison

The results presented in this section contain the full development of the COPV model, *i.e.* the model includes the six layers of cohesive elements on both metal-composite and CFRP interfaces to predict delamination. Fig. 5 shows the comparison of the experimental Model C cylinder behaviour and the FE result. It is observed that the FE model correlates well to the experimental curve as it predicts the main features of the *F-d* behaviour. The initial elastic response is well correlated although there are some differences that can be attributed to noise, as no delamination was observed at indenter displacements of less than 1 mm. The first slope change, related to the metal yielding, is also well predicted by the FE model. The curve shows a good correlation with the predicted peak force having a 6.2% difference to the experimental value. Similar to the elastic response, noise is noticeable in this region

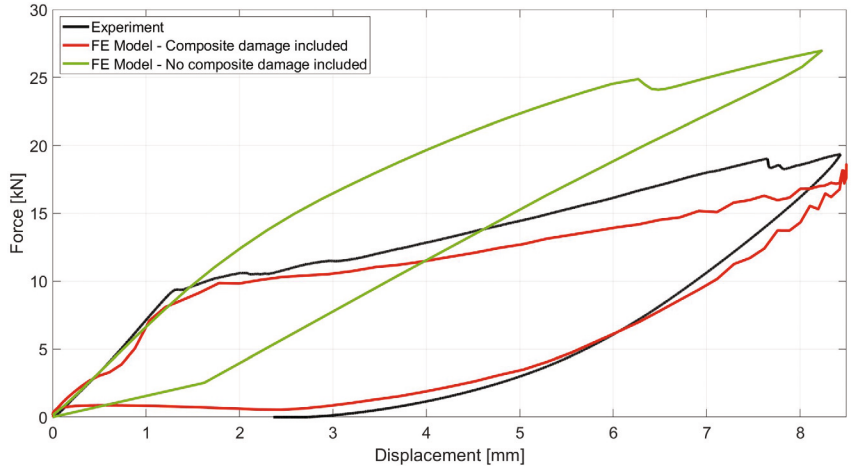

Fig. 6. Effect of modelling the composite delamination on the structural response of the Type III cylinder FE model.

of the curve, however this can be attributed to the delamination occurring at multiple interfaces of the model. Thus, for this particular section of the curve, the model is not only predicting the structural behaviour but the damage occurring in the composite, which was also reported in the experimental results [11]. The unloading behaviour is also well captured by the FE model. It can be observed that both model and experiment show a similar response. Additionally, it was also observed that modelling delamination within the composite layers has a noticeable effect on the overall structural response. Fig. 6 suggests that the main contributions of the composite layers delamination model is the change of slope after yielding and the unloading response, in which the residual dent shape is ultimately developed.

Using this model it is also possible to observe permanent deformation progression in the metal liner as well as damage propagation in the different interfaces. Fig. 7 shows the development of the residual dent in the aluminium liner compared to specific points on the *F-d* curve. Point *A* shows the onset of metal yielding with a 3.1% plastic deformation of the liner. Point *B* shows an intermediate point between the initial loading and maximum indentation. It is possible to observe that the plastic deformation of the liner has increased up to 7.8% along with some delamination. The plastic strain exhibited at point *C* is similar to that shown at the end of the load application (point *D*) which is 13.2% and 13.1% respectively. This results suggests that for Model C, once the maximum load has been applied, the deformation of the metal liner has reached its maximum extent. This could be considered as a guide for robust design purposes focusing on reducing the maximum displacement allowed by the liner under maximum load application.

Along with dent development, damage propagation in the individual interfaces can be explored using the FE model. Fig. 8 shows different levels of damage observed in the delamination region where the cohesive elements were defined. Similar to the indentation analysis, each level of delamination is related to a specific section of the *F-d* curve. Each image shows the outermost layer and the innermost layer, where the former is the top cohesive interface layer of the CFRP material and the latter is the metal-composite cohesive interface. Point *A* shows no delamination during the onset of aluminium yielding, thus, being in the elastic response region suggests no significant damage to the structure. The intermediate Point *B* shows some level of delamination in the top and the metal-composite interface. From the bottom view, it is observed different extents of delamination occur at the individual ply interfaces, where the metal-composite cohesive layer delamination has the greatest extent. In contrast to the plastic strain development in the liner, Points *C* and *D* on Fig. 8 exhibit a significant difference in the results. Delamination levels between those points are different despite having a similar deformation in the liner. The main difference between these two points is the region that has been damaged. Point *C* corresponds to the maximum compression being applied to the structure, as such, it is suggested that the observed damage here was developed under mode II delamination. Moreover, Point *D* damage corresponds to complete load removal from the cylinder and the residual dent being fully developed. At these regions of the curve, it can be observed that cohesive elements on the centre, (*i.e* elements directly under the indenter) have been also removed, which suggests that delamination occurred in mode I. Results reported in [11] suggested that metal-composite decohesion would occur during the unloading stage of the experiment under mode I as a consequence of the elastic recovery of the composite whilst the liner has been permanently deformed. Results shown by the FE model suggest that this is true for some regions of the indentation area, however there is also extensive damage occurring in mode II delamination during the loading stage. This delamination behaviour is consistent with the results reported in previous work [12].

Following quantitative validation of the full cylinder model, measurement of residual indentation was performed. Fig. 9a shows the residual indentation depth predicted by the FE model, which is 5.09 mm. The value reported in previous work [11] is $\approx$ 4.3 mm, which would make the FE estimate have an error of 15.5%. A more direct qualitative comparison between the CT scan and the FE resulting residual dents is shown in Fig. 9b and c. The overall comparison is qualitatively good, with similar shapes of the deformed material and extents of the damage. The key difference appears to be that in the experiment there is an undamaged region immediately under the indenter, which is presumably the result of crushing and high through thickness compressive stresses which act to suppress delamination. This is likely to be the main source of the discrepancy between the model predictions and experimental measurement of the dent depth.

Delamination area measurements were also reported in [11]. The value for a Model C cylinder is $\approx$ 2500 mm^2 at a $\approx$ 20 kN peak force. Although this is approximate, this measurement offers an idea of the delamination extension, which can be then compared to the FE model predictions. For a clearer reference to the reader, each layer in the model has been named as described in Fig. 10. Fig. 10a shows a view of the model's solid element layers in which each material is indicated. Fig. 10b shows the cohesive element layers, layer L1 corresponds to the metal-composite interface layer, and layers L2-L5 correspond to the composite interface layers. Fig. 11 shows that delamination occurred on every interface layer of Model C, although the extent of delamination is different for each layer. Fig. 11a & b exhibit the projected area of delamination from L5 and L1 respectively. This comparison shows that the extent of delamination on the former is larger than the latter. Such differences in the area of delamination between each layer are the result of the different fibre direction of the plies, and are consistent with

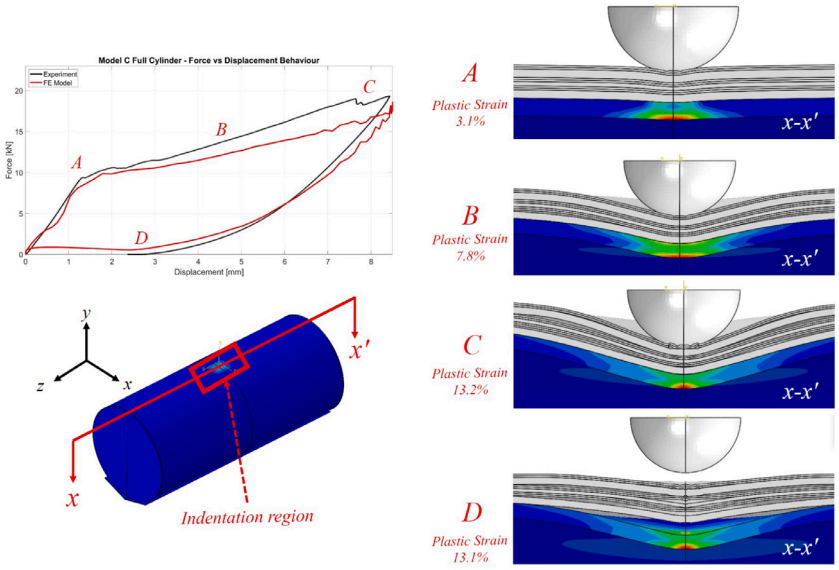

Fig. 7. Residual dent development in the metal liner of Model C Type III cylinder.

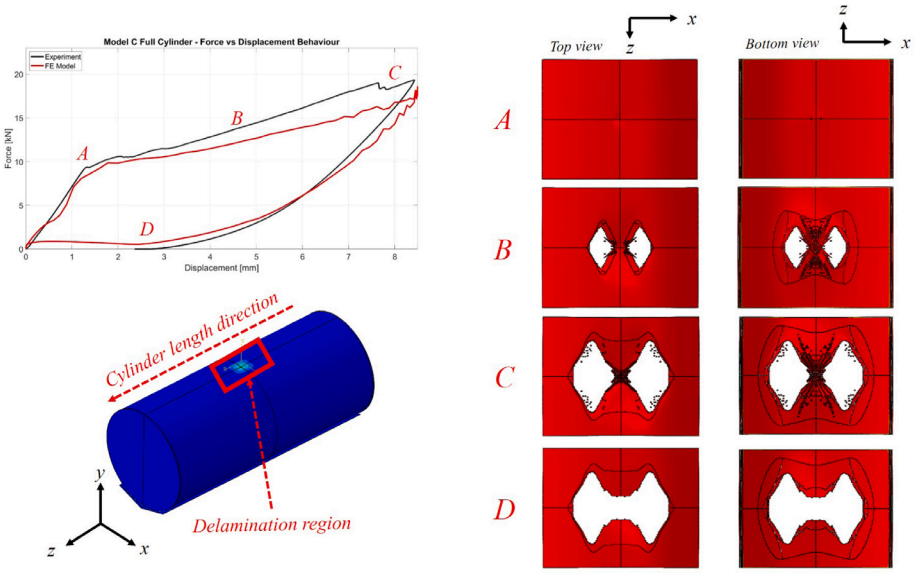

Fig. 8. Delamination propagation at the metal-composite interface and composite ply interfaces in a model of a type III cylinder.

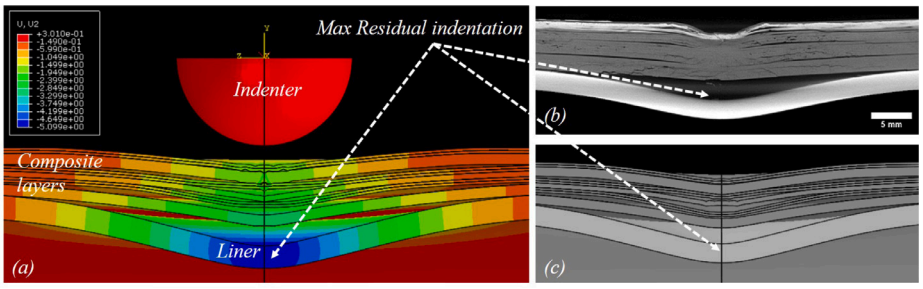

Fig. 9. Residual dent in Model C cylinder after load removal; (a) FE dent depth result, (b) CT scan indentation [11], (c) FE indentation.

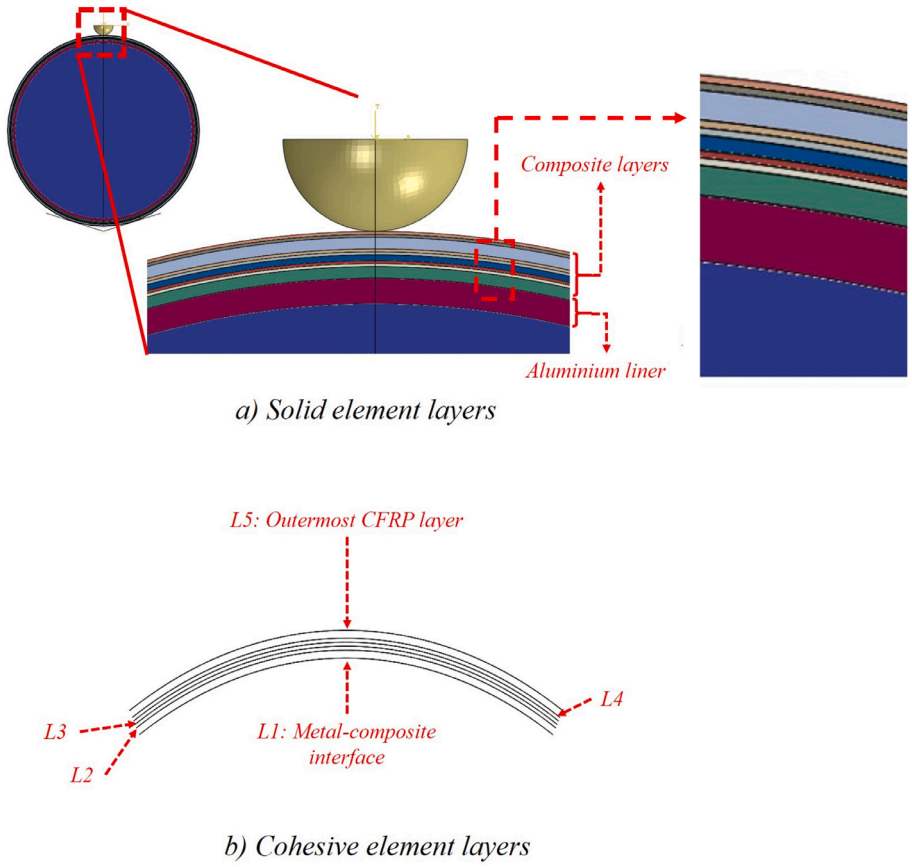

Fig. 10. Cohesive element interface layers within the Type III cylinder model.

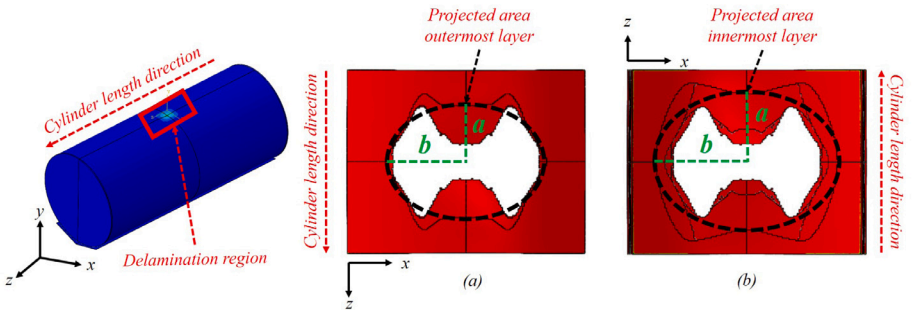

Fig. 11. Model C delamination after quasi-static loading; (a) Outermost CFRP layer, (b) Metal-composite interface.

observations of the extent of delaminations through the thickness in composite plates subject to quasi-static indentation [16]. In both cases, an estimation of the projected area was performed to compare versus the experimental values. The projected area considered is defined by the smallest ellipse that encompasses the delamination at a particular interface and is described in Fig. 11. For the outermost layer, the calculated area is 1508 mm^2 and for the innermost area (metal-composite interface) the estimated value is 2073 mm^2.

3.2. Model implementation on different composite overwrap pressure vessel geometries

The current model aims to be used for design exploration purposes and, as such, the model must be proven to be reliable given changes in design parameters, *i.e.* different geometry, materials or constructions can be explored with the model using the same cohesive parameters for the metal-composite interface. To test the reliability of the model to geometric changes, more simulations were performed using the COPV models described in Section 2.1. A python script was created to automate the pre-processing activities related to model generation such as creating the geometry, materials and boundary conditions.[1] For Model A, Model B and Model D cylinders no liner dent depth was reported in [11], thus FE results are compared only to experimental *F-d* curves. Fig. 12 shows the FE to experimental comparison for these cylinder types. All cylinders have the same end plate thickness (2 mm). Regarding the cohesive element region (finer mesh area), each cylinder has also ≈ 20% of the total length populated with cohesive elements, except for Model D which had to be extended to ≈ 30%. These models were run similarly to Model C, on the Iridis supercomputer using 32 CPUs. Details of number of elements and simulation time are described on Table 2.

[1] Full script can be access upon request via University of Southampton repository https://doi.org/10.5258/SOTON/D1635.

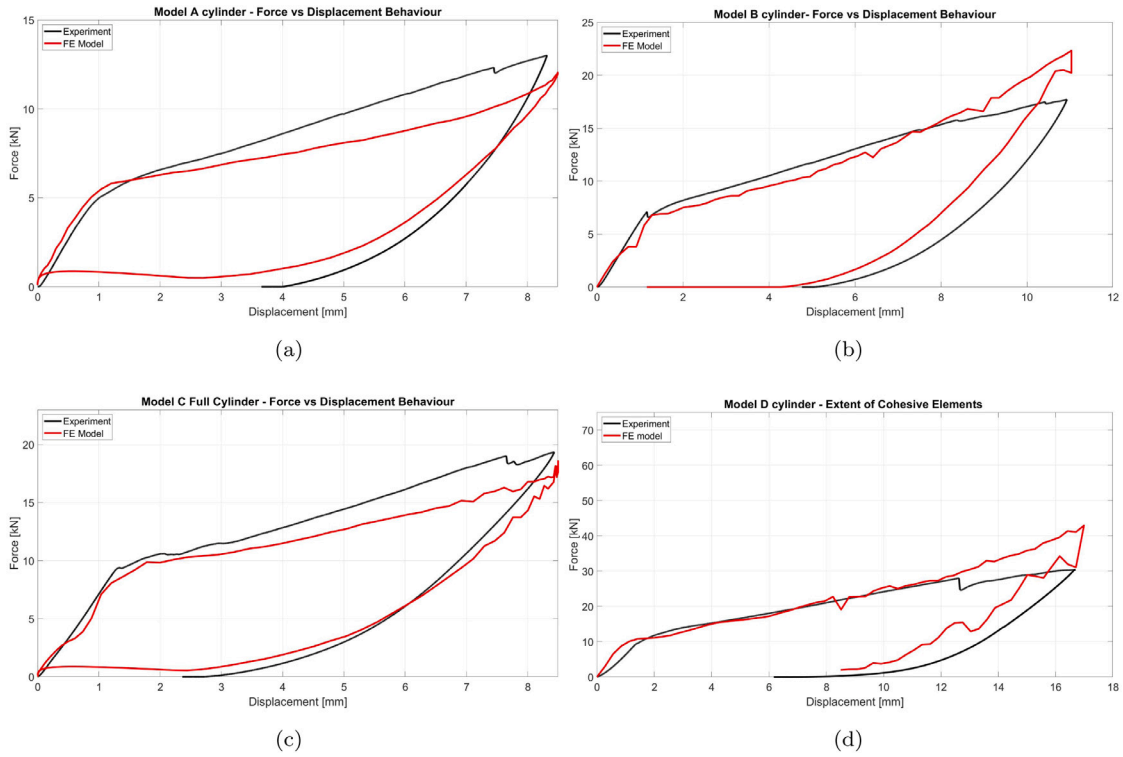

Fig. 12. Comparison of experimental and FE force–displacement curves of different Type III cylinders.

Model A shows a similar behaviour to that exhibited by Model C with acceptable correlation between the FE and experimental *F-d* curve. The total error regarding the peak force is ≈ 7%. In contrast, models B and D show an over prediction of peak force towards the end of the loading stage. The error is ≈ 20% and ≈ 28% respectively. As suggested in Section 3.1, as the thickness of the CFRP layers increases the effect of the damage on these is higher, that is why Model A showed a good correlation to the experimental values on the loading part of the curve without having composite delamination included in the model. The results presented in this section show a similar behaviour with respect to the number of cohesive layers contained in the cylinders. For instance, the overestimation of stiffness exhibited on the *F-d* curves from Model B and D corresponds to the reduced number of cohesive layers (4) modelled compared to Model A (6). The lack of delamination in the composite implies less energy dissipation through composite damage, hence, resulting in a stiffer structure. This effect could be reduced if more cohesive layers or matrix/fibre damage were included in future models.

4. Summary & conclusions

A methodology to implement cohesive elements into a COPV has been described in this paper. Moreover, this numerical model has been applied to a range of cylinder designs with different geometries and good correlation between simulation and experimental results has been demonstrated. It was shown that interface properties previously estimated provide a good model-to-experiment correlation when implementing them in a full COPV. Validation of this was provided through comparison of the *F-d* curves, residual dent depth and delamination area measurements. All the cylinder models described and investigated in this chapter showed good correlations when compared to experimental *F-d* curves. In each case, prediction of the initial elastic response, material yielding (first slope change), similar peak force and non-elastic unloading response were shown. Additionally, in the case of Model C cylinder, results showed good correlation values for the residual dent measurement and the projected delamination area, which was also confirmed with qualitative comparison between FE results and a CT scan image. Therefore, it was concluded that it is possible to use the same interface properties in various cylinder designs without any additional calibration. Overall, it was concluded that the methodology presented in this paper can be used to develop FE models to explore design opportunities for COPV as the interface parameters used have been tested under different design conditions and the validity of results has been demonstrated. Although the results presented in this paper are specific to a particular set of cylinders produced by a particular manufacturer, using a particular process, the approach taken is quite general, and could be transferred to other comparable cylinder designs (*i.e.* Type III cylinders).

Overall the approach taken represents a further example of the benefit of combining advanced numerical modelling with sophisticated imaging techniques, such as computed tomography. The ability to explore damage and deformation in 3D with high resolution provides greatly enhanced abilities to calibrate and validate numerical models; elsewhere this has been referred to as “Data Rich Mechanics”. Additionally, having numerical models with such capabilities can reduce product’s development time and costs by minimizing the amount of testing required to validate engineering designs.

CRediT authorship contribution statement

Erick Montes de Oca Valle: Investigation. **S.M. Spearing:** Supervision. **Ian Sinclair:** Supervision. **Trevor Allen:** Investigation. **Warren Hepples:** Supervision.

Declaration of competing interest

The authors Erick Montes de Oca Valle, Mark Spearing, Ian Sinclair, Warren Hepples & Trevor Allen declare that they have no competing financial interests or personal relationships that could have appeared to influence the work reported in this paper.

Data availability

The data that has been used is confidential.

Acknowledgements

We would like to thank Luxfer Gas Cylinders for their financial support and constant help, which was key to success in the achievement of this publication. We also want to thank the National Council for Science and Technology (CONACYT) in Mexico, for the financial support provided, which made possible the development of this research.

References

[1] H. Barthelemy, M. Weber, F. Barbier, Hydrogen storage: Recent improvements and industrial perspectives, Int. J. Hydrogen Energy 42 (11) (2017) 7254–7262, http://dx.doi.org/10.1016/j.ijhydene.2016.03.178.

[2] S. Wakayama, S. Kobayashi, T. Imai, T. Matsumoto, Evaluation of burst strength of FW-FRP composite pipes after impact using pitch-based low-modulus carbon fiber, Composites A 37 (11) (2006) 2002–2010, http://dx.doi.org/10.1016/j.compositesa.2005.12.010.

[3] M. Weber, C. Devilliersa, N. Guillaud, F. Dau, B. Gentilleauc, F. Nony, S. Villalonga, D. Halm, Damage tolerance of compressed gaseous hydrogen composites vessels, in: 16th European Conference on Composite Materials, ECCM 2014, 2014, pp. 22–26, (June).

[4] Y.-S. Kim, L.-H. Kim, J.-S. Park, The effect of composite damage on fatigue life of the high pressure vessel for natural gas vehicles, Compos. Struct. 93 (11) (2011) 2963–2968, http://dx.doi.org/10.1016/j.compstruct.2011.05.007.

[5] Z. Changliang, R. Mingfa, Z. Wei, C. Haoran, Delamination prediction of composite filament wound vessel with metal liner under low velocity impact, Compos. Struct. 75 (1–4) (2006) 387–392, http://dx.doi.org/10.1016/j.compstruct.2006.04.012.

[6] M.-G. Han, S.-H. Chang, Failure analysis of a Type III hydrogen pressure vessel under impact loading induced by free fall, Compos. Struct. 127 (2015) 288–297, http://dx.doi.org/10.1016/j.compstruct.2015.03.027, URL http://linkinghub.elsevier.com/retrieve/pii/S0263822315001993.

[7] M.G. Han, S.H. Chang, Evaluation of structural integrity of Type-III hydrogen pressure vessel under low-velocity car-to-car collision using finite element analysis, Compos. Struct. 148 (2016) 198–206, http://dx.doi.org/10.1016/j.compstruct.2016.03.060.

[8] G. Perillo, F. Grytten, S. Sørbø, V. Delhaye, Numerical/experimental impact events on filament wound composite pressure vessel, Composites B 69 (2015) 406–417, http://dx.doi.org/10.1016/j.compositesb.2014.10.030.

[9] J. Zheng, Y. Hu, L. Ma, Y. Du, Delamination failure of composite containment vessels subjected to internal blast loading, Compos. Struct. 130 (2015) 29–36, http://dx.doi.org/10.1016/j.compstruct.2015.04.013.

[10] R.A. Weerts, O. Cousigné, K. Kunze, M.G. Geers, J.J. Remmers, Assessment of contact-induced damage mechanisms in thick-walled composite cylinders, J. Reinf. Plast. Compos. 39 (17–18) (2020) 679–699, http://dx.doi.org/10.1177/0731684420923043.

[11] T.M. Allen, Damage Development and Post-Impact Performance of Composite Overwrapped Pressure Vessels Subjected to Low Velocity Impact (Ph.D. thesis), University of Southampton, 2017.

[12] E. Montes de Oca Valle, M. Spearing, I. Sinclair, W. Hepples, T. Allen, Model-experiment comparison for transverse loading of metal-composite ring specimen (Part 1), Compos. Struct. (2021).

[13] T. Allen, S. Ahmed, W. Hepples, P.A. Reed, I. Sinclair, M. Spearing, A comparison of quasi-static indentation and low-velocity impact on composite overwrapped pressure vessels, J. Compos. Mater. 52 (29) (2018) 4051–4060, http://dx.doi.org/10.1177/0021998318774401.

[14] D.S. Son, S.H. Chang, Evaluation of modeling techniques for a type III hydrogen pressure vessel (70 MPa) made of an aluminum liner and a thick carbon/epoxy composite for fuel cell vehicles, Int. J. Hydrogen Energy 37 (3) (2012) 2353–2369, http://dx.doi.org/10.1016/j.ijhydene.2011.11.001.

[15] P.W. Harper, S.R. Hallett, Cohesive zone length in numerical simulations of composite delamination, Eng. Fract. Mech. 75 (16) (2008) 4774–4792, http://dx.doi.org/10.1016/j.engfracmech.2008.06.004.

[16] D. Liu, E. Lansing, L.E. Malvern, Cracking in impacted glass / epoxy plates, J. Compos. Mater. 21 (July 1987) (1987) 594–609.